HPC for the study of health issues resulting from the exposure of humans to electromagnetic fields

Tristan Cabel and Stéphane Lanteri

NACHOS project-team, INRIA Sophia Antipolis - Méditerranée
06902 Sophia Antipolis Cedex, France
Stephane.Lanteri@inria.fr

International Conference for
High Performance Computing, Networking, Storage and Analysis (SC10)
New Orleans, Louisiana, November 13-19, 2010

Societal context

Year	2003	2004	2005	2006	2007	2008	2009
# users ($\times 10^6$)	41.6	43.8	48.1	51.7	55.4	58.1	61.4
% active population	69.1	72.6	78.4	80.8	85.6	89.1	95.8

As of 2008,

- 71% of 12-14 years old kids owned a mobile phone,
- 95% coverage of the 15-17 years olds.

ElectroMagnetic (EM) waves in our environment

- Natural sources (earth magnetic field, etc.)
- Manmade sources
  - Domestic appliances: TV, radio, microwave ovens, hairdryers, fridges, etc.
  - Technological devices: mobile phones, Wi-Fi, etc.

Characterization of EM fields and related effects

- An EM field is characterized by its frequency (Hz, MHz, GHz)
- Ionising radiation
  - Upper part of the frequency spectrum
  - Can induce changes at the molecular level
  - x-rays and gamma rays
- Non-ionising radiation
  - Lower part of the frequency spectrum
  - Static and power frequency fields, radiofrequencies, microwaves and infrared radiation

Basic physiological processes

- Energy from radio-frequency fields is absorbed into the body

$$\text{SAR (Specific Absorption Rate): } \frac{\sigma|\mathbf{E}|^2}{\rho}$$

- Energy is converted to heat
- Energy is dissipated by the body's normal thermoregulatory process

Health issues related to hand-held mobile phones

- Biological effects versus sanitary effects
  - Biological effects: physiological, biochemical or behavioral changes induced in a body, tissue or cell by an external source
  - A biological effect does not necessarily represent a risk for human health
  - Sanitary effects: consequences of biological effects that change the normal behavior of a body
- Thermal effects versus non-thermal effects
  - A thermal effect results from a local or systemic heating of a tissue
  - Thermal effects are relatively well known
  - Ongoing studies are concerned with non-thermal effects

Health issues related to hand-held mobile phones

- Epidemiological studies
  - Possible links with various cancers
- Experimental studies
  - Dosimetry of animal exposure
  - In vivo and in vitro studies
- Computer simulation studies
  - Numerical dosimetry of EM fields
    - Maxwell equations for space-time evolution of the electromagnetic field $(\mathbf{E}, \mathbf{H})$
    - Electromagnetic characteristics of the propagation media
      ε, σ and ρ are varying accross tissues
      They also depend on the frequency of the signal
    - Discontinuities of **E** and **H** occur at interfaces between different tissues
  - Evaluation of temperature elevation in tissues
    - Bioheat equation for the steady state temperature

Cartesian grid methods (FDTD : Finite Difference Time Domain)

- Advantages
  - Easy computer implementation
  - Computationally efficient (very low algorithmic complexity)
  - Mesh generation is straightforward (medical images are voxel based)
  - Modelization of complex sources (antennas, thin wires, etc.) is well established
- Drawbacks
  - Accuracy on non-uniform discretizations
  - Memory requirements for high resolution models
  - Approximate discretization of boundaries (staircase representation)
- FDTD is the prevalent approach for the numerical dosymetry analysis of mobile phone radiation
  - P. Bernardi *et al.* (U. La Sapienza, Roma, Italy)
  - O.P. Gandhi *et al.* (U. of Utah, USA)
  - J. Wiart *et al.* (FTR&D, France)
  - etc.

Motivations

Numerical dosimetry of EM fields: unstructured grid methodologies

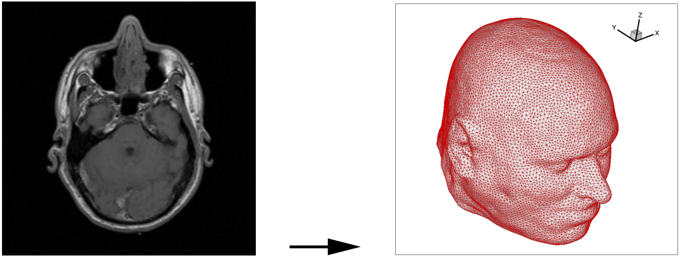

Geometric models

- Built from segmented medical images
- Extraction of surfacic (triangular) meshes of the tissue interfaces using specific tools
    - Marching cubes + adaptive isotropic surface remeshing
    - Delaunay refinement
- Generation of tetrahedral meshes using a Delaunay/Voronoi tool

Computational electromagnetics

- Challenges with the simulation of electromagnetic (EM) wave propagation in biological tissues
  - Geometrical characteristics of the propagation domain:
    - dimensions relatively to the wavelength,
    - irregularly shaped objects and singularities.
  - Physical characteristics of the propagation medium:
    - heterogeneity and anisotropy,
    - physical dispersion and dissipation.
  - Characteristics of the radiating sources and incident fields

James Clerk Maxwell (1831-1879)

Modeling context

Overall objective of this study and numerical approach

- Development of a flexible and efficient finite element simulation tool adapted to hybrid CPU-GPU parallel systems for the study of 3D electromagnetic wave propagation problems in complex domains and heterogeneous media
- Application to the numerical dosimetry of EM fields
  - Industrial partner: Orange Labs (Joe Wiart, Issy-les-Moulineaux, France)
- Numerical ingredients
  - Unstructured meshes (triangles in 2D, tetrahedra in 3D)
  - Discontinuous Galerkin Time-Domain method with polynomial interpolation (DGTD-$\mathbb{P}_p$ method)
    - Can easily deal with discontinuous coefficients and solutions
    - Can handle unstructured, non-conforming meshes
    - Yield local finite element mass matrices
    - High order accurate methods with compact stencils
    - Naturally lead to discretization (h-) and interpolation order (p-) adaptivity
    - Amenable to efficient parallelization
  - Explicit time stepping

Time-domain Maxwell equations

$$\begin{cases} \varepsilon\partial_t \mathbf{E} - \nabla\times\mathbf{H} = 0 \\ \\ \mu\partial_t \mathbf{H} + \nabla\times\mathbf{E} = 0 \end{cases}$$

$$\mathbf{E} = {}^{\mathrm{T}}(E_x, E_y, E_z) \text{ and } \mathbf{H} = {}^{\mathrm{T}}(H_x, H_y, H_z)$$

Weak formulation

- Triangulation of Ω: $\overline{\Omega_h} \equiv \mathscr{T}_h = \bigcup\limits_{\tau_i\in\mathscr{T}_h} \overline{\tau}_i$
- Approximation space: $V_h = \{\mathbf{V}_h \in L^2(\Omega)^3 \mid \forall i, \mathbf{V}_{h|\tau_i} \equiv \mathbf{V}_i \in \mathbb{P}_{p_i}(\tau_i)^3\}$

$$\begin{cases} \displaystyle\iiint_{\tau_i} \vec{\varphi}\cdot\varepsilon_i\partial_t\mathbf{E}_i d\omega = \frac{1}{2}\iiint_{\tau_i}(\nabla\times\vec{\varphi}\cdot\mathbf{H}_i + \nabla\times\mathbf{H}_i\cdot\vec{\varphi})d\omega - \frac{1}{2}\sum_{k\in\mathscr{V}_i}\iint_{a_{ik}}\vec{\varphi}\cdot(\mathbf{H}_k\times\vec{n}_{ik})ds \\ \displaystyle\iiint_{\tau_i} \vec{\varphi}\cdot\mu_i\partial_t\mathbf{H}_i d\omega = -\frac{1}{2}\iiint_{\tau_i}(\nabla\times\vec{\varphi}\cdot\mathbf{E}_i + \nabla\times\mathbf{E}_i\cdot\vec{\varphi})d\omega + \frac{1}{2}\sum_{k\in\mathscr{V}_i}\iint_{a_{ik}}\vec{\varphi}\cdot(\mathbf{E}_k\times\vec{n}_{ik})ds \end{cases}$$

Global EDO system

$$\mathbf{M}^{\varepsilon}\frac{d\mathbb{E}}{dt} = \mathbf{G}\mathbb{H} \quad \text{and} \quad \mathbf{M}^{\mu}\frac{d\mathbb{H}}{dt} = -{}^{\mathsf{T}}\mathbf{G}\mathbb{E}$$

- $\mathbf{G} = \mathbf{K} - \mathbf{A} - \mathbf{B}$
- $\mathbf{M}^{\varepsilon}$ are $\mathbf{M}^{\mu}$ block diagonal symmetric definite positive matrices
- $\mathbf{K}$ is a block diagonal symmetric matrix
- $\mathbf{A}$ is a block sparse symmetric matrix
- $\mathbf{B}$ is a block sparse skew symmetric matrix

Leap-Frog based explicit time integration

$$\begin{cases} \mathbf{M}^{\varepsilon}\left(\dfrac{\mathbb{E}^{n+1} - \mathbb{E}^{n}}{\Delta t}\right) & = & \mathbf{G}\mathbb{H}^{n+\frac{1}{2}} \\ \mathbf{M}^{\mu}\left(\dfrac{\mathbb{H}^{n+\frac{3}{2}} - \mathbb{H}^{n+\frac{1}{2}}}{\Delta t}\right) & = & -{}^{\mathsf{T}}\mathbf{G}\mathbb{E}^{n+1} \end{cases}$$

Implementation

The DGTD method is an iterative algorithm that computes at each time step the evolution of the electric and magnetic fields

Each iteration can be decomposed into 4 steps applied at the tetrahedron level

intVolume : computes the volume integral,

$$\frac{1}{2}\iiint_{\tau_i}(\nabla\times\vec{\varphi}\cdot\mathbf{H}_i+\nabla\times\mathbf{H}_i\cdot\vec{\varphi})d\omega$$

intSurface : computes the surface integral for internal faces $a_{ik}=\tau_i\cap\tau_j$,

$$\frac{1}{2}\sum_{k\in\mathscr{V}_i}\iint_{a_{ik}}\vec{\varphi}\cdot(\mathbf{H}_k\times\vec{n}_{ik})ds$$

IntSurfaceBdry : computes the surface integral (same as above) for boundary faces

UpdateEM : updates the electromagnetic field

Initial implementation for CPU based systems

intVolume : loop over mesh elements τ_i

$$\mathbf{F}_{\tau_i} = \frac{1}{2} \iiint_{\tau_i} (\nabla \times \vec{\varphi} \cdot \mathbf{H}_i + \nabla \times \mathbf{H}_i \cdot \vec{\varphi}) d\omega$$

$\Rightarrow$ Update flux balance of element τ_i

intSurface and IntSurfaceBdry : loop over mesh faces $a_{ik} = \tau_i \cap \tau_j$

$$\mathbf{F}_{a_{ik}} = -\mathbf{F}_{a_{ki}} = \frac{1}{2} \sum_{k \in \mathcal{V}_i} \iint_{a_{ik}} \vec{\varphi} \cdot (\mathbf{H}_k \times \vec{n}_{ik}) ds$$

$\Rightarrow$ Update flux balance of elements τ_i and τ_j

UpdateEM : loop over mesh elements τ_i

$\Rightarrow$ Exploit flux balance of element τ_i

Development of DG kernels in CUDA

Specific adaptations for GPU computing

- Perform intSurface and IntSurfaceBdry at the element level
  $\Rightarrow$ Implies redundant calculation of $\mathbf{F}_{a_{ik}}$ and $\mathbf{F}_{a_{ki}}$
- All operations are now implemented as loops over mesh elements

A remake of the past

C. Farhat, L. Fezoui and S. Lanteri
Two-dimensional viscous flow computations on the connection machine: unstructured meshes, upwind schemes, and massively parallel computations
Comput. Meth. App. Mech. Engng., Vol. 102, 1993

Parallelization strategy for clusters of CPUs

Domain partitioning + message passing programming (MPI)

Performance assessment

Computing platform

HPC resource mad available by GENCI (Grand Equipement National de Calcul Intensif)
Allocation 2010-t2010065004

Hybrid CPU-GPU cluster of the CCRT (Centre de Calcul Recherche et Technologie)
in Bruyères-le-Châtel, France

1068 Intel CPU nodes with two quad-core Intel Xeon X5570 Nehalem processors
operating at 2.93 GHz each

48 Teslas S1070 GPU systems with four GT200 GPUs and two PCI Express-2 buses each

The network is a non-blocking, symmetric, full duplex Voltaire InfiniBand double data rate
organized as a fat tree

The original DGTD software is developed in Fortran 90

Simulations are performed in single precision arithmetic

Weak scalability

Model test problem and configurations

Propagation of a standing wave in a perfectly conducting unitary cubic cavity

Regular uniform tetrahedral meshes respectively containing 3,072,000 elements for the DGTD-$\mathbb{P}_1$ and DGTD-$\mathbb{P}_2$ methods, 1,296,000 elements for the DGTD-$\mathbb{P}_3$ method and 750,000 elements for the DGTD-$\mathbb{P}_4$ method

Boxwise domain decompositions with optimal computational load balance

Timings for 1000 iterations and up to 128 GPUs

Weak scalability: timings

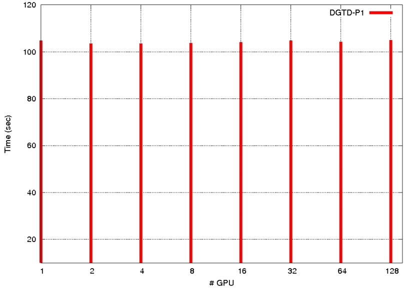

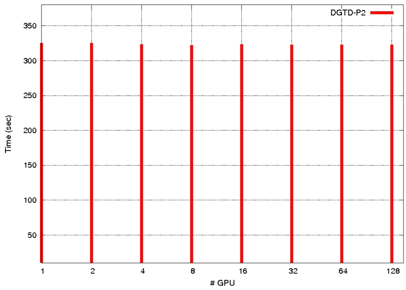

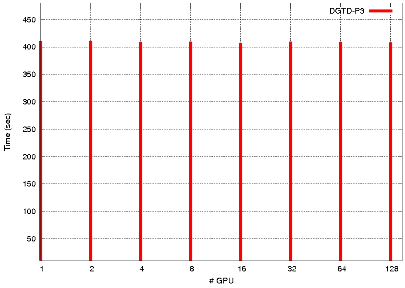

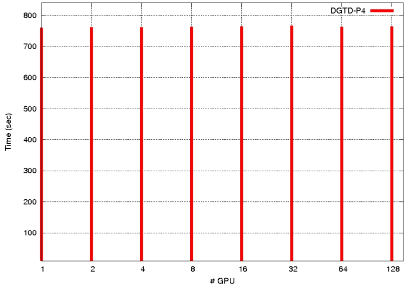

Weak scalability: GFlops rates

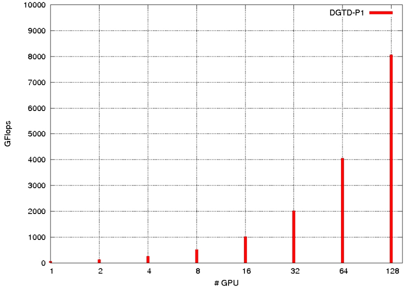

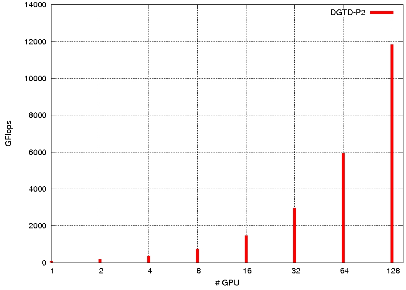

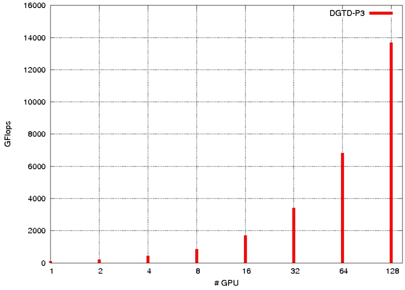

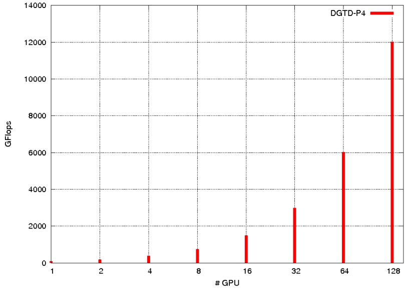

Weak scalability

Model test problem and congiurations

Propagation of a standing wave in a perfectly conducting unitary cubic cavity

Regular uniform tetrahedral meshes respectively containing 3,072,000 elements for the DGTD-$\mathbb{P}_1$ and DGTD-$\mathbb{P}_2$ methods, 1,296,000 elements for the DGTD-$\mathbb{P}_3$ method and 750,000 elements for the DGTD-$\mathbb{P}_4$ method

Boxwise domain decomposition with optimal computational load balance

Timings for 1000 iterations and up to 128 GPUs

Computational performances

# GPU	DGTD-$\mathbb{P}_1$	DGTD-$\mathbb{P}_2$	DGTD-$\mathbb{P}_3$	DGTD-$\mathbb{P}_4$
1	63 GFlops	92 GFlops	106 GFlops	94 GFlops
128	8072 GFlops	11844 GFlops	13676 GFlops	12009 GFlops

Strong scalability

Head tissues exposure to mobile phone radiation

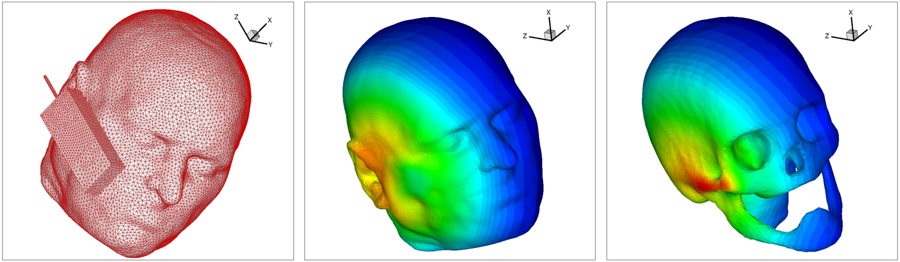

- Mesh: # elements = 7,894,172
- Total # dof is 189,45,8688 (DGTD-$\mathbb{P}_1$ method) and 473,646,720 (DGTD-$\mathbb{P}_2$ method)
- Time on 128 CPU cores: 2786 sec (DGTD-$\mathbb{P}_1$ method) and 6057 sec (DGTD-$\mathbb{P}_2$ method)

# GPU	DGTD-$\mathbb{P}_1$			DGTD-$\mathbb{P}_2$		
	Time	GFlops	Speedup	Time	GFlops	Speedup
32	162 sec	146	-	816 sec	2370	-
64	97 sec	2470	1.7	416 sec	4657	2.0
128	69 sec	3469	2.4	257 sec	7522	3.2

Strong scalability

Women with foetus

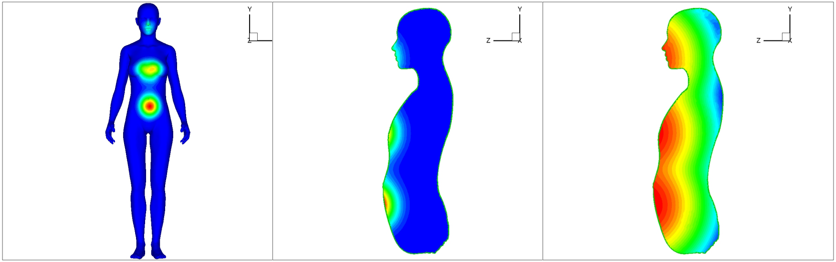

- Mesh: # elements = 5,536,852
- Total # dof is 132,884,448 (DGTD-$\mathbb{P}_1$ method) and 332,211,120 (DGTD-$\mathbb{P}_2$ method)
- Time on 64 CPU cores for the DGTD-$\mathbb{P}_1$ method: 7 h 10 mn

# GPU	DGTD-$\mathbb{P}_1$			DGTD-$\mathbb{P}_2$		
	Time	GFlops	Speedup	Time	GFlops	Speedup
64	12 mn	2762	-	59 mn	4525	-
128	7 mn	4643	1.7	30 mn	8865	1.95

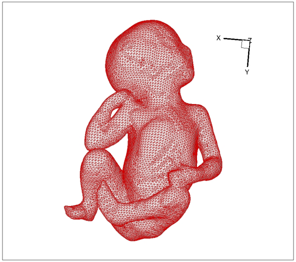

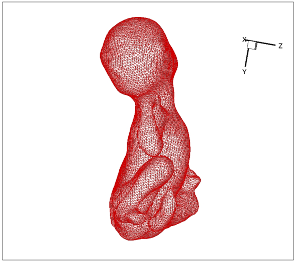

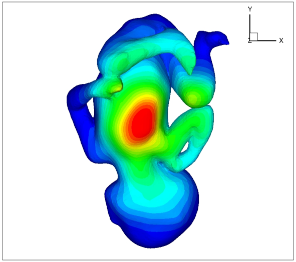

- Mesh: # elements = 5,536,852
- Total # dof is 132,884,448 (DGTD-$\mathbb{P}_1$ method) and 332,211,120 (DGTD-$\mathbb{P}_2$ method)
- Time on 64 CPU cores for the DGTD-$\mathbb{P}_1$ method: 7 h 10 mn

# GPU	DGTD-$\mathbb{P}_1$			DGTD-$\mathbb{P}_2$		
	Time	GFlops	Speedup	Time	GFlops	Speedup
64	12 mn	2762	-	59 mn	4525	-
128	7 mn	4643	1.7	30 mn	8865	1.95